Wavelength-Dependent Photolysis of Methylglyoxal in the 290−440 nm Region

Yunqing Chen, Wenjing Wang,† and Lei Zhu*

Wadsworth Center, New York State Department of Health, Department of Environmental Health and Toxicology, State University of New York, Albany, New York 12201-0509

Received: June 22, 2000

Photodissociation of methylglyoxal (CH_3COCHO; MGLY) in the 290−440 nm region has been investigated at 10 nm intervals by using dye laser photolysis in combination with cavity ring-down spectroscopy. Absorption cross sections of methylglyoxal were obtained at each wavelength studied. The HCO radical was a photodecomposition product. The formation yield of HCO, determined by monitoring its absorption at 613.8 nm, decreased with increasing MGLY pressure in the 1−10 Torr range. The HCO yields (extrapolated to zero MGLY pressure) were unity in the 320−360 nm region, consistent with the photodissociation mechanism $CH_3COCHO + h\nu \rightarrow CH_3CO + HCO$ (P1). The HCO yields decreased at both the shorter (290−310 nm) and the longer (370−440 nm) wavelength end. The dependence of the HCO yields on nitrogen buffer gas pressure was also examined. The HCO radical yields were independent of nitrogen pressure (10−400 Torr) between 290 and 370 nm, but decreased with increasing nitrogen pressure in the 380−440 nm region. The coefficients for the dependence of the HCO radical yields on MGLY pressure and total pressure were given. Absorption cross sections and quantum yields thus obtained were used to calculate atmospheric photodissociation rate constants and lifetimes of MGLY as a function of zenith angle for cloudless conditions at sea level and at 760 Torr nitrogen pressure. Photolysis lifetimes of MGLY were on the order of 1.4−2.3 h for zenith angles in the 0−60° range.

Introduction

The atmospheric chemistry of methylglyoxal (CH_3COCHO; MGLY) has been a subject of substantial interest because MGLY is a major product from ozonolysis and OH-initiated oxidation of isoprene.[1−8] It has been detected from air-photooxidation of methyl-substituted aromatic hydrocarbons in the presence of NO_x.[9,10] Concentrations of MGLY on the order of 50 pptv have been observed in the field.[11,12]

Photolysis and OH radical reactions have been identified as the major gas-phase loss processes for MGLY.[13−15] A rate constant[15] for OH radical reaction of 1.3×10^{-11} cm^3 $molecule^{-1}$ s^{-1} was reported at room temperature, which corresponds to an OH radical reaction lifetime of 23 h using an average OH concentration of 10^6 molecules cm^{-3}. Photolysis lifetimes were estimated from the absorption cross sections of MGLY and its average photolysis quantum yields.[13,14,16,17] Absorption cross section data were reported by Plum et al.,[16] Meller et al.,[18] and Staffelbach et al.[14] There is good agreement between cross section values obtained by Meller et al.[18] and by Staffelbach et al.[14] Photolysis product studies published by Raber and Moortgat[13] and by Staffelbach et al.[14] were conducted by using broadband excitation and FTIR detection. A number of photodissociation pathways are thermodynamically allowed[17,19] following electronic excitation of MGLY in the near UV and visible region:

$$CH_3COCHO + h\nu \rightarrow CH_3CO + HCO \ (\lambda \leq 414 \text{ nm}) \quad \text{(P1)}$$

$$\rightarrow CH_3COCO + H \ (\lambda \leq 384 \text{ nm}) \quad \text{(P2)}$$

$$\rightarrow CH_3 + COCHO \ (\lambda \leq 369 \text{ nm}) \quad \text{(P3)}$$

$$\rightarrow CH_3 + CO + HCO \ (\lambda \leq 343 \text{ nm}) \quad \text{(P4)}$$

$$\rightarrow CH_3CO + H + CO \ (\lambda \leq 337 \text{ nm}) \quad \text{(P5)}$$

$$\rightarrow CH_3CHO + CO \ (\text{all } \lambda) \quad \text{(P6)}$$

$$\rightarrow CH_4 + CO + CO \ (\text{all } \lambda) \quad \text{(P7)}$$

Following the analysis of stable products such as CO, CO_2, H_2-CO, CH_3OH, HCOOH, CH_3COOH, CH_3COO_2H, O_3, H_2O, etc., after the photolysis of MGLY in air, Raber and Moortgat[13] and Staffelbach et al.[14] proposed that the major photolysis pathway of MGLY in the actinic UV region is $CH_3COCHO + h\nu \rightarrow CH_3CO + HCO$. Significant differences exist in the average photolysis quantum yields reported by these two studies, which translates into a factor of 5 difference in the atmospheric photodissociation lifetime of MGLY. Recently, Koch and Moortgat[17] measured the photodissociation quantum yields of MGLY by monitoring the stable end products CO and HCHO as a function of wavelength ($260 \leq \lambda \leq 320$ nm; $380 \leq \lambda \leq 440$ nm) and pressure ($30 \leq \lambda \leq 900$ Torr) using an optical resolution of 8.5 nm. Photolysis quantum yields of unity, independent of wavelength and pressure, were reported in the 260−320 nm region. Photolysis quantum yields were found to decrease with increasing wavelength and pressure in the 380−440 nm region. In view of the large difference in the MGLY photolysis quantum yields determined by various investigations, we have directly measured the wavelength-dependent HCO radical formation yields from the photodissociation of MGLY by using laser photolysis in combination with cavity ring-down spectroscopy.[20,21]

Reported in this paper are results obtained from the photolysis of MGLY at 10 nm intervals in the 290−440 nm region.

* Corresponding author. E-mail: zhul@orkney.ph.albany.edu.
† Current address: Department of Physics and Astronomy, University of Toledo, Toledo, OH 43606.

10.1021/jp002262t CCC: $19.00
Published on Web 10/27/2000

Absorption cross sections of MGLY were measured at each wavelength studied. The HCO radical yields were determined as a function of MGLY pressure and total pressure. The absolute HCO radical concentration was calibrated relative to those obtained from formaldehyde (H_2CO) photolysis or from the Cl + $H_2CO \rightarrow$ HCl + HCO reaction. Photodissociation lifetimes of MGLY were calculated as a function of zenith angle for cloudless conditions at sea level and at 760 Torr nitrogen pressure.

Experimental Section

The experimental apparatus has been described in detail elsewhere.[22−24] Photolysis radiation was provided by a tunable dye laser pumped by a XeCl excimer laser (∼180 mJ/pulse). Both the fundamental (340−440 nm) and the second harmonic (290−330 nm) output of the dye laser were used. The fundamental dye laser output was attenuated in order to prevent multiphoton dissociation. Typical laser fluence used in the experiments was in the range 0.005−0.015 J cm^{-2}. Laser dyes used to cover the 290−330 nm region included Rhodamine 6G, Rhodamine B, Rhodamine 101, Sulfurhodamine 101, and DCM. Laser dyes used in the 340−440 nm range were *p*-Terphenyl, DMQ, QUI, Stilbene 3, and Coumarin 120. The photodissociation light pulse propagated into the reaction cell at a 15° angle with the main cell axis through a sidearm, while the probe light pulse (613−617 nm) from a nitrogen-pumped dye laser was introduced along its main optical axis. The photolysis and the probe laser beams were overlapped at the center of the reaction cell vacuum-sealed with a pair of high-reflectance (∼99.999% at 614 nm) cavity mirrors. A fraction of the probe laser output was injected into the cavity through the front mirror. The photon intensity decay inside the cavity was monitored by measuring the weak transmission of light through the rear mirror with a photomultiplier tube (PMT). The PMT output was amplified, digitized, and transferred to a computer. The decay curve was fitted to a single-exponential decay function and the total loss per optical pass was calculated. By measuring cavity losses with and without a photolysis pulse, HCO absorption from the photolysis of MGLY was obtained. The photolysis laser pulse energy was determined with a calibrated joulemeter.

Gas pressure at the center of the reaction cell was monitored with a baratron capacitance manometer. Quantum yield measurements were performed at a laser repetition rate of 0.1 Hz to ensure replenishment of the gas sample between successive laser shots. Spectral scans were carried out at a laser repetition rate of 1 Hz. All measurements were made at an ambient temperature of 293 ± 2K.

MGLY, which was obtained commercially as a 40% solution in water (Aldrich), was vacuum pumped overnight in a flask covered with a black cloth in order to remove water and to prevent slow photolysis of MGLY by room light. The resulting highly viscous hydrated MGLY was covered with a 2 cm thick layer of phosphorus pentoxide (purum; ≥98% purity; Fluka), and then it was distilled at 50−60 °C and 10^{-3} Torr. MGLY vapor was trapped at ethanol−dry ice temperature (−78.5 °C) as a green-yellowish liquid with a viscosity comparable to that of water. Freshly prepared MGLY was pumped at the temperature of dry ice for at least 30 min before use to remove impurities such as CO, H_2CO, and acetic acid from the sample.

Formaldehyde was generated by pyrolysis of polymer paraformaldehyde (≥95% purity; Aldrich) at 110 °C. Nitrogen (≥ 99.999% purity; Praxair) and Cl_2 (≥ 99.5% purity; Matheson) were used without further purification.

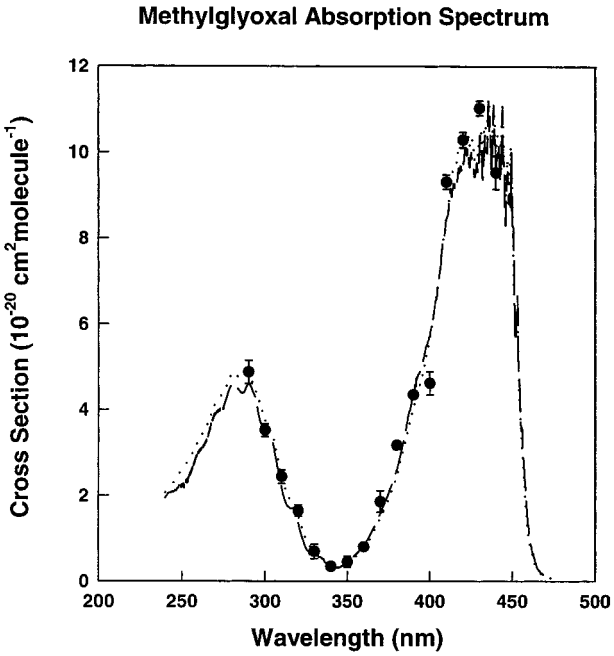

Figure 1. Absorption spectrum of methylglyoxal at room temperature. Circles: cross sections determined in this work. Dotted line: those reported by Meller et al. Dashed line: those reported by Staffelbach et al. Error bars are ±1σ.

TABLE 1: Absorption Cross Sections of Methylglyoxal as a Function of Wavelength

λ (nm)	σ (10^{-20} cm^2 $molecule^{-1}$)
290	4.88 ± 0.27
300	3.52 ± 0.15
310	2.44 ± 0.16
320	1.65 ± 0.13
330	0.70 ± 0.15
340	0.32 ± 0.04
350	0.48 ± 0.11
360	0.80 ± 0.06
370	1.80 ± 0.22
380	3.17 ± 0.10
390	4.35 ± 0.08
400	4.62 ± 0.27
410	9.31 ± 0.17
420	10.29 ± 0.18
430	11.03 ± 0.17
440	9.53 ± 0.39

Results and Discussion

Absorption Cross Sections of MGLY in the 290−440 nm Region. The absorption cross sections of MGLY were determined at room temperature at 10 nm intervals in the 290−440 nm region. They are shown in Figure 1 and listed in Table 1. The absorption spectrum of MGLY displayed two bands in the near UV and visible region as a result of two different n → π^* transitions.[25,26] The absorption cross section at each wavelength was obtained by monitoring the transmitted photolysis photon intensity as a function of MGLY pressure in the cell and by applying Beer's law to the data obtained. Error bars quoted (1σ) are the estimated precision of cross section determination, which includes the standard deviation for each measurement (∼0.5%) plus the standard deviation about the mean of at least four repeated experimental runs. Besides random errors, systematic errors also contribute to the uncertainty in cross section values. The major sources of systematic errors are those involving pressure (0.1%) and path-length (0.2%) determinations, and those due to the presence of impurity (<2%) in MGLY. Adding relative (see Table 1) and systematic errors, the overall

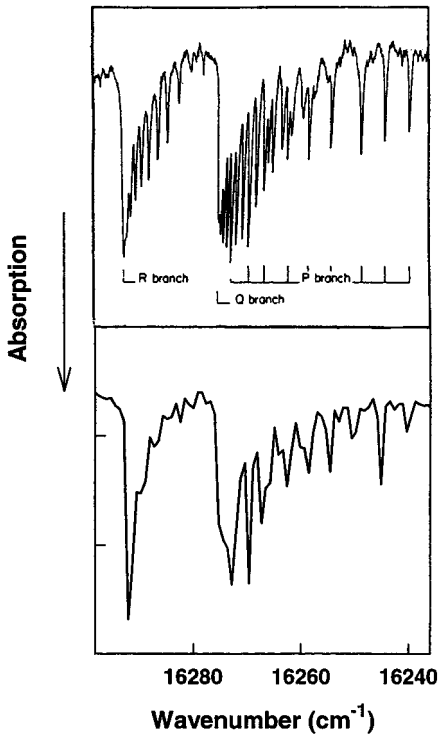

Figure 2. Lower trace: low resolution cavity ring-down absorption spectrum of the product from 290 nm photolysis of 5.5 Torr MGLY. Upper trace: intracavity laser absorption spectrum of the (000) → (090) vibronic transition of HCO following photolysis of 0.1 Torr CH_3CHO/10 Torr Ar at 266 nm (adapted from ref 27).

uncertainty in cross-section measurements is ∼10% for all wavelengths except for 330, 340, 350, and 370 nm, where the size of the cross section is small. Estimated overall uncertainty in cross section values are ∼24%, 16%, 26%, and 15% at 330, 340, 350, and 370 nm. Included in Figure 1 for comparison are cross-section results obtained by Meller et al.[18] and by Staffelbach et al.[14] Except for the data points at 380 and 400 nm, there is a good agreement between our cross section values and those obtained by Meller et al.[18] and by Staffelbach et al.[14] Our cross section values at 380 and 400 nm are about 20% different from those obtained from the previous studies.

HCO Radical Yields from the Photolysis of MGLY in the 290−440 nm Region. Shown in Figure 2 is a cavity ring-down absorption spectrum of the product from the 290 nm photolysis of MGLY measured at a pump/probe laser delay of 15 μs in the 613−618 nm region. Also shown in the same figure is a previously reported absorption spectrum[27] of the HCO radical in the same wavelength region. A comparison of these two spectra indicates that the HCO radical is a photolysis product of MGLY. The cavity ring-down spectrometer was tuned to the HCO $X^2A''(0,0,0) \rightarrow A\ ^2A'(0,9,0)$ R bandhead at 613.8 nm, and HCO radical yields from the photolysis of MGLY were determined. The HCO radical yield was derived from the ratio of the HCO concentration produced in the photolysis/probe laser overlapping region to the absorbed photon density in the same region. The overlapping region could be regarded as a rectangular solid with width and height defined by those of the photolysis beam, and length defined by (beam width) × $\tan(15°)^{-1}$, where 15° is the angle between the photolysis and the probe beams. Absorption of the photolysis beam by MGLY in the pump/probe laser overlapping region could be derived from the difference in the transmitted photon intensity at the beginning and at the end of the overlapping region. Once we know the incident photon energy into the cell and the absorption cross section of MGLY at the photolysis wavelength, we could calculate the absorbed photon density in this overlapping region for a given initial MGLY pressure. The photolysis photon energy incident into the cell was measured with a joulemeter calibrated by acetone photolysis actinometry.[28] The HCO concentration resulting from the photolysis can be determined by measuring its absorption at 613.80 nm at a photolysis/probe laser delay of 15 μs. To convert HCO absorption into absolute concentration, the absorption cross section of HCO at the probe laser wavelength was determined relative to that obtained from formaldehyde photolysis for which the HCO quantum yield is known[29] and/or from the $Cl + H_2CO \rightarrow HCO + HCl$ reaction. Formaldehyde photolysis was used as a calibration standard when photolysis studies were conducted in the 290−310 nm region. H_2CO was prepared in a gas bulb prior to each calibration run. The purity of H_2CO was estimated by comparing its absorption cross sections with literature values.[30,31] The absorption cross section of H_2CO was determined by measuring the transmitted photolysis photon intensity as a function of H_2CO pressure in the cell and by applying Beer's law to the data obtained. Our H_2CO cross section values at 290 and 300 nm agree within ±20% with those obtained by Moortgat et al.[30] Our H_2CO cross section at 310 nm is $(1.02 \pm 0.11) \times 10^{-20}$ cm^2 $molecule^{-1}$, which is 35% smaller than the extrapolated literature value[31] of 1.58×10^{-20} cm^2 $molecule^{-1}$. The previous study was conducted at 2.5 nm interval and was centered at a different wavelength. The difference in cross section values between the present and the previous study may reflect a difference in the spectral resolution of these two studies. The $Cl + H_2CO$ reaction was used to calibrate the absolute HCO concentration when photolysis studies were conducted at 290 nm and in the 310−440 nm region. To ensure all Cl atoms generated from the photolysis of chlorine ($Cl_2 + h\nu \rightarrow 2Cl$) reacted with H_2CO, Cl_2 and H_2CO were introduced into the cell at $P_{Cl_2}/P_{H_2CO} = 1/5$. Absorption cross sections of Cl_2 were determined at the photolysis wavelengths. They agreed with literature values[32] within 5−10% at 290, 310, 320, 430 nm; within 11−20% in the 330−390 nm region; about 23% at 400, 420 nm; about 27% at 440 nm. At 290 and 310 nm, both formaldehyde photolysis and the $Cl + H_2CO$ reaction were used as references to calibrate absolute HCO concentration. The HCO absorption cross section obtained by these two methods agreed within 5% at 290 nm and within 14% at 310 nm. Since the probe laser bandwidth is broader than the HCO linewidth, the HCO cross section values were dependent on the wavelength resolution of our probe laser system.

The HCO radical yields from the photolysis of MGLY at 1, 2, 4, 6, 8, and 10 Torr MGLY pressure were measured. Shown in Figure 3 is a plot of the HCO radical yield from the 290 nm photolysis of MGLY as a function of MGLY pressure. As can be seen, the HCO radical yields decreased with increasing MGLY pressure possibly due to the quenching of the excited precursor to dissociation by MGLY and to HCO + HCO and CH_3CO + HCO radical−radical reactions. To extract the zero MGLY pressure HCO radical yield (φ_{HCO}^0), the reciprocal HCO yields were plotted against MGLY pressure according to the Stern−Volmer relation:

$$1/\varphi_{HCO} = 1/\varphi_{HCO}^{\ 0} + k_{MGLY}^{\ Q} \cdot P_{MGLY}$$

where k_{MGLY}^{Q} is the quenching rate constant by MGLY. Shown in Figure 4 is a Stern−Volmer plot of the reciprocal HCO yields from 290 nm photolysis of MGLY. A linear relationship was observed from the plot. The coefficients φ_{HCO}^0 and k_{MGLY}^{Q} as a function of the photolysis wavelength are listed in Table 2

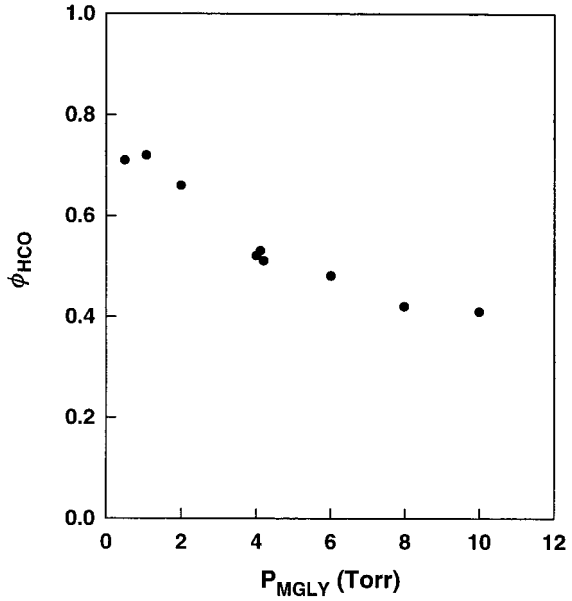

Figure 3. The HCO radical yields as a function of MGLY pressure from the photolysis of MGLY at 290 nm.

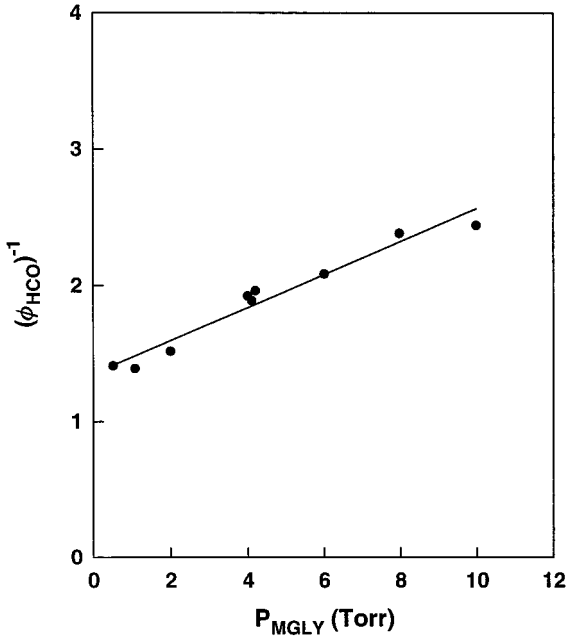

Figure 4. Stern−Volmer plot of the reciprocal HCO yields from 290 nm photolysis of MGLY as a function of MGLY pressure. Circles: experimental data; solid line: fit to the Stern−Volmer expression.

(both φ_{HCO}^0 and k_{MGLY}^Q) and plotted in Figure 5 (φ_{HCO}^0 only). The error bars include the standard deviation of the parameters obtained from the least-squares fit of the Stern−Volmer plot plus the run-to-run variations. The systematic errors include uncertainties in the determination of the following parameters: HCO absorption cross section and thus absolute HCO concentration (∼20% in the 290−430 nm region; ∼27% at 440 nm), MGLY concentration (∼2%), MGLY absorption cross section (10% for all wavelengths except for 330, 340, 350, 370 nm; 24%, 16%, 26%, 15% at 330, 340, 350, 370 nm), pulse energy (5%), and the dye laser width. Since the HCO radical yields from the photolysis of MGLY were determined relative to those obtained from H_2CO photolysis or from the $Cl + H_2CO$ reaction, uncertainty in the determination of the dye laser width should not affect the relative yield measurement. The overall uncertainty in φ_{HCO}^0 measurements were 37% at 360 nm, in the 290−320 nm and 380−430 nm regions, 42−44% at 340, 370, and 440 nm, and 51−53% at 330 and 350 nm. As seen from Figure 5, the coefficients φ_{HCO}^0 are unity in the 320−360 nm region, consistent with the photodissociation mechanism $CH_3COCHO + h\nu \rightarrow CH_3CO + HCO$ (P1). At $\lambda \leq 310$ nm, the photolysis quantum yields decreased with decreasing wavelength, suggesting the occurrence of an additional photodissociation process such as $CH_3COCHO + h\nu \rightarrow CH_3CO + H + CO$ at higher photon energies. The HCO radical yields decreased with increasing wavelength in the 370−440 nm region consistent with dissociation at near threshold wavelengths and also the occurrence of nondissociative processes such as fluorescence and phosphorescence in competition with photodissociation. We observed light emission when photolysis studies were conducted in the 380−440 nm region. Such light emission remained even milliseconds after the firing of the photolysis laser. If the light emission were not filtered out, we would observe the fortuitous increase in HCO radical yields with increasing aldehyde pressure in the 380−440 nm region. Therefore, a red pass filter was used to filter out the emitted light.

Koch and Moortgat[17] reported a methylglyoxal photolysis quantum yield (φ_0) of unity in the 260−380 nm region. Since their study was conducted in air and they could not distinguish

TABLE 2: The Coefficients φ^0_{HCO} and k_{MGLY}^Q from the Photolysis of Methylglyoxal as a Function of Wavelength

λ(nm)	φ^0_{HCO}	k_{MGLY}^Q
290	0.82 ± 0.06	0.079 ± 0.023
300	0.89 ± 0.07	0.056 ± 0.015
310	0.88 ± 0.08	0.088 ± 0.018
320	0.97 ± 0.08	0.055 ± 0.014
330	1.02 ± 0.19	0.14 ± 0.04
340	1.16 ± 0.20	0.047 ± 0.019
350	1.13 ± 0.17	0.12 ± 0.03
360	1.01 ± 0.11	0.081 ± 0.018
370	0.86 ± 0.07	0.096 ± 0.016
380	0.92 ± 0.10	0.18 ± 0.03
390	0.89 ± 0.11	0.27 ± 0.02
400	0.56 ± 0.09	0.46 ± 0.05
410	0.32 ± 0.03	0.38 ± 0.04
420	0.27 ± 0.04	0.59 ± 0.05
430	0.20 ± 0.04	0.61 ± 0.11
440	0.17 ± 0.02	0.48 ± 0.06

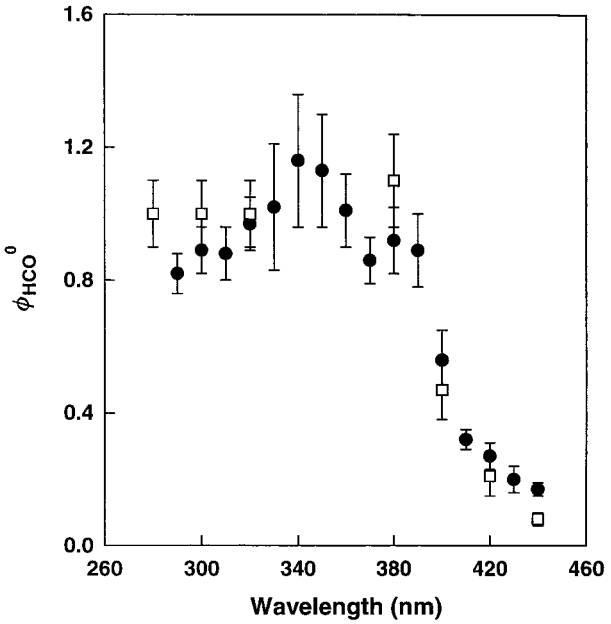

Figure 5. Circles: zero-pressure HCO radical yields from the photolysis of MGLY as a function of photodissociation wavelength. Squares: zero-pressure MGLY photolysis quantum yields reported by Koch and Moortgat.

photodissociation processes such as $CH_3COCHO + h\nu \rightarrow CH_3CO + HCO$ (P1) and $CH_3COCHO + h\nu \rightarrow CH_3CO + H + CO$, our φ_{HCO}^0 values of less than unity at $\lambda \leq 310$ nm do not necessarily indicate a discrepancy between our results and theirs. They reported total photolysis quantum yields (φ_0) of 1.10 ± 0.14, 0.47 ± 0.09, 0.21 ± 0.06, and 0.08 ± 0.02 at 380, 400, 420, and 440 nm. Our φ_{HCO}^0 values are 0.86 ± 0.07, 0.92 ± 0.10, 0.89 ± 0.11, 0.56 ± 0.09, 0.32 ± 0.03, 0.27 ± 0.04, 0.20 ± 0.04, 0.17 ± 0.02 at 370, 380, 390, 400, 410, 420, 430, and 440 nm. There is a good agreement between our zero-pressure HCO yields and their zero-pressure MGLY photolysis yields at 380, 400, and 420 nm, but not at 440 nm. φ_0 values obtained by Koch and Moortgat at $\lambda > 380$ nm can be described by an exponential function of the reciprocal wavelength using the following equation:

$$\varphi_0(\lambda) = (8.15 \pm 0.5)(10^{-9})[\exp((7131 \pm 267)/\lambda)]>$$

Applying a similar analysis to our φ_{HCO}^0 values in the 390−440 nm region would result in the following expression:

$$\varphi_{HCO}{}^0(\lambda) = (3.63 \pm 0.32)(10^{-7})[\exp((5693 \pm 533)/\lambda)]$$

To explain the independence of H_2CO yields from the photolysis of MGLY in air in the 400−440 nm region, Koch and Moortgat[17] proposed the occurrence of a minor process in addition to photodissociation pathway (P1). This minor process was intermolecular H-atom transfer between electronically excited MGLY and ground-state MGLY

$$[CH_3CHO]^* + CH_3CHO \rightarrow CH_3CO + H_2CO + CO + CH_3CO \quad \text{(R1)}$$

There was no evidence from our study that the HCO radical was formed from such H-atom transfer process between electronically excited and ground-state MGLY.

The dependence of the HCO radical yields on total pressure was examined by maintaining a constant MGLY pressure and varying the nitrogen carrier gas pressure. The HCO radical yields were found to be independent of total pressure (8−400 Torr) in the 290−370 nm region, but decreased with increasing pressure in the 380−440 nm region. Displayed in Figure 6 is a plot of the reciprocal HCO yields from the 390 nm photolysis of MGLY as a function of nitrogen pressure. The slope of such a plot gives the quenching coefficient of the excited MGLY by nitrogen ($k_{N_2}^Q$) at 390 nm. $k_{N_2}^Q$ values in the 380−440 nm region were given in Table 3. The errors represent the standard deviation of the least-squares fit of the $1/\varphi_{HCO}$ vs P_{N_2} plot. Using coefficients $k_{N_2}^Q$ and φ_{HCO}^0 determined in this work, the HCO radical yields from the photolysis of MGLY at 760 Torr N_2 pressure were extrapolated and they are listed in Table 3. Also included in Table 3 for comparison are the previously reported total photolysis quantum yields of MGLY in the 380−440 nm region and in 760 Torr air by Koch and Moortgat.[17] The ratio of our HCO yields and their total photolysis quantum yields are 1.4, 2.4, 3.2, and 4.9 at 380, 400, 420, and 440 nm. Koch and Moortgat fit their k_{air}^Q in the 400−440 nm region with an exponential function of the negative reciprocal wavelength of the following form:

$$k_{air}{}^Q = (1.36 \pm 0.02) \times 10^8\,[\exp(-(8793 \pm 300)/\lambda)]$$

The following expression was obtained when a similar analysis was applied to our $k_{N_2}^Q$ values in the 380−440 nm region:

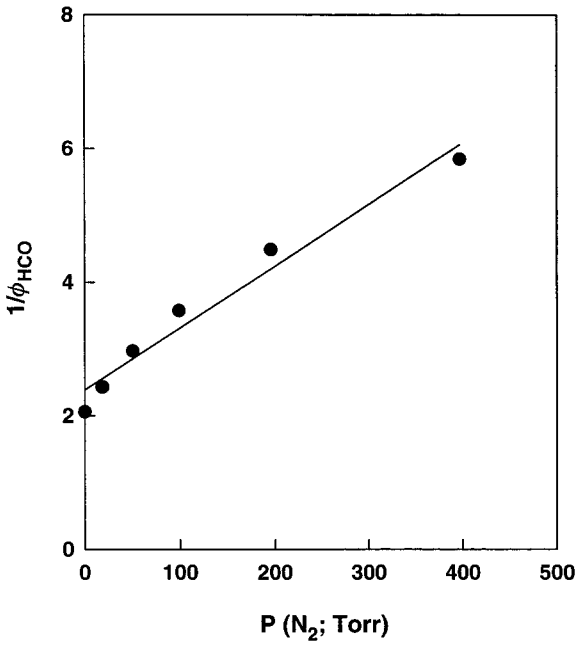

Figure 6. Stern−Volmer plot of the reciprocal HCO yields from the 390 nm photolysis of 2 Torr MGLY as a function of nitrogen pressure. Circles: experimental data; solid line: fit to the Stern−Volmer expression.

TABLE 3: The Coefficients $k_{N_2}^Q$ from the Photolysis of Methylglyoxal in Nitrogen as a Function of Wavelength

λ(nm)	$k_{N_2}^Q$	$\varphi_{HCO}^{760\ Torr}$ (this work)	$\varphi_0^{760\ Torr}$ (Koch)
380	0.008 ± 0.002	0.13	0.094
390	0.009 ± 0.001	0.12	
400	0.012 ± 0.001	0.090	0.038
410	0.022 ± 0.001	0.050	
420	0.030 ± 0.003	0.038	0.012
430	0.046 ± 0.011	0.025	
440	0.046 ± 0.004	0.024	0.0049

$$k_{N_2}{}^Q = (1.93 \pm 0.24) \times 10^4\,[\exp(-(5639 \pm 497)/\lambda)]$$

Staffelbach et al.[14] measured photolysis quantum yields of MGLY in 760 Torr air using broadband excitation and they were 0.14, 0.055, and 0.005 in the 240−420, 355−480, and 410−418 nm region. Our $\varphi_{HCO}^{760\ Torr}$ averaged over the 355−480 and 410−418 nm region would be 0.19 and 0.046, larger than those obtained by Staffelbach et al.[14] Raber and Moortgat determined methylglyoxal photolysis quantum yield in air (54−760 Torr) using broadband filter in the 275−380 nm and 390−470 nm region. The quantum yields were 0.64 ± 0.03 and 0.23 ± 0.02 in the 275−380 nm and 390−470 nm region and in 760 Torr air. Our HCO yield averaged over 390−470 nm region and at 760 Torr N_2 pressure was 0.035.

Searching for CH_3CO. Attempts were made to search for a possible visible absorption band of CH_3CO as a result of its similar electronic structure compared with HCO. CH_3CO exhibits a UV absorption band,[33,34] but its visible absorption spectrum has not been reported. The photolysis study was conducted at 410 nm at which fragmentation of CH_3CO into $CH_3 + CO$ was not expected to occur. The probe laser was scanned over the wavelength region 570−670 nm. No structured absorption attributable to CH_3CO was observed.

Photodissociation Rate Constants To Form HCO Radicals. The photodissociation rate constant of MGLY to form HCO (k_{rad}) was calculated from the actinic solar flux ($J(\lambda)$) reported by Demerjian et al.,[35] the absorption cross sections ($\sigma(\lambda)$) of MGLY, and the HCO radical yields at 760 Torr N_2 pressure

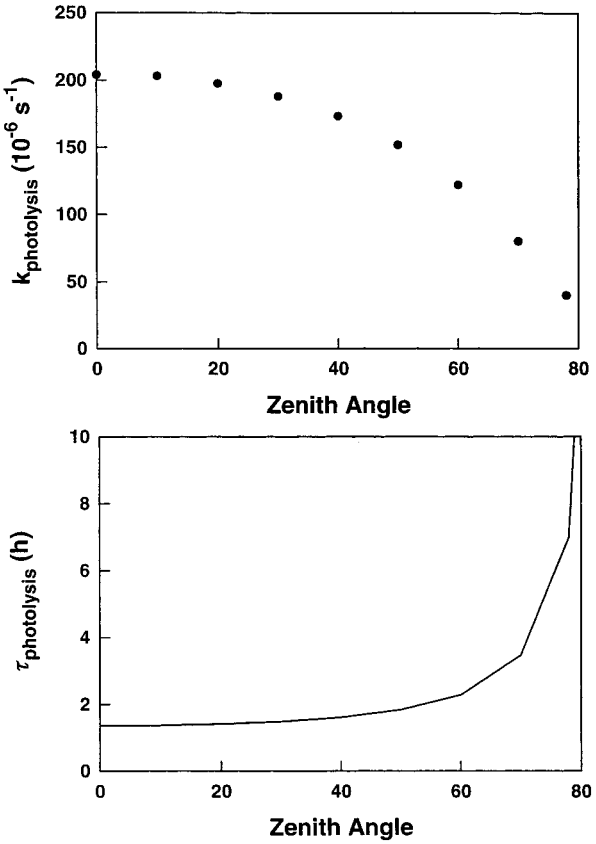

Figure 7. Atmospheric photodissociation rate constants (upper figure) and lifetimes (lower figure) of MGLY as a function of zenith angle under cloudless conditions at sea level and at 760 Torr nitrogen pressure.

($\phi_{HCO}^{760\ Torr}$) using the following relationship:

$$k_{rad} = \int \boldsymbol{J}(\lambda)\cdot\sigma(\lambda)\cdot(\phi_{HCO}^{760\ Torr})\ d\lambda$$

Since formation of $CH_3CO + HCO$ is the dominant MGLY photolysis pathway in the actinic UV region, the photolysis rate constant of MGLY to form HCO is approximately equal to its total photolysis rate constant. Atmospheric photodissociation rate constants and lifetimes of MGLY were calculated as a function of zenith angle under cloudless conditions at sea level and for best estimate albedo, and the results are shown in Figure 7. Our estimated MGLY photolysis lifetimes were on the order of 1.4−2.3 h for zenith angles in the 0−60° range. Photolysis lifetimes of MGLY were given by several previous investigations. Plum et al.[16] used an unfiltered Xe lamp to simulate the solar spectrum and reported a photolysis lifetime of 2 h. Raber and Moortgat[13] gave an estimated lifetime value of 0.6 h using a photolysis quantum yield of 0.23 obtained with a broadband emission source in the 390−470 nm region. Staffelbach et al.[14] reported a photolysis lifetime of 2.7 h by assuming that the MGLY photolysis quantum yield decreased linearly with wavelength from a value of 0.45 at 300 nm to a value of 0 at 430 nm and by assuming half of the MGLY loss in their experiments was due to reaction with HO_2. Koch and Moortgat[17] calculated the MGLY photolysis lifetime as a function of zenith angle for 0.5 km height, and gave a value of 4.1 h for a zenith angle of 50°. Thus our MGLY photolysis lifetimes agree within a factor of 2 with those reported by Plum et al., by Staffelbach et al., and by Koch and Moortgat.

Conclusions

We have investigated photodissociation of methylglyoxal in the 290−440 nm region by using dye laser photolysis in combination with cavity ring-down spectroscopy. Absorption cross sections of methylglyoxal were obtained. The HCO radical was a photolysis product of MGLY. The dependence of the HCO yields on MGLY pressure and total pressure was examined, and explicit expressions for such dependence were provided. Absorption cross section and quantum yield results were used to calculate MGLY photolysis lifetimes (1.4−2.3 h) as a function of zenith angle (0−60°) in the atmosphere.

Acknowledgment. We thank Mr. Vu Q. Huynh for his assistance in the experiments. We are grateful to Dr. Geoffrey S. Tyndall for many helpful discussions and for providing hints on methylglyoxal synthesis. This work was supported by National Science Foundation under Grant No. ATM-9610285 and by the Petroleum Research Fund under Grant No. 32261AC6.

References and Notes

(1) Killus, J. P.; Whitten, G. Z. *Environ. Sci. Technol*. **1984**, *18*, 142.
(2) Paulson, S. E.; Flagan, R. C.; Seinfeld, J. H. *Int. J. Chem. Kinet.* **1992**, *24*, 79.
(3) Kamens, R. M.; Gery, M. W.; Jeffries, H. E.; Jackson, M.; Cole, E. I. *Int. J. Chem. Kinet.* **1982**, *14*, 955.
(4) Niki, H.; Maker, P. D.; Savage, C. M.; Breitenbach, L. P. *Environ. Sci. Technol.* **1983**, *17*, 312A.
(5) Paulson, S. E.; Flagan, R. C.; Seinfeld, J. H. *Int. J. Chem. Kinet.* **1992**, *24*, 103.
(6) Tuazon, E. C.; Atkinson, R. *Int. J. Chem. Kinet.* **1990**, *22*, 591.
(7) Tuazon, E. C.; Atkinson, R. *Int. J. Chem. Kinet.* **1989**, *21*, 1141.
(8) Atkinson, R.; Aschmann, S. M.; Winer, A. M.; Pitts, J. N., Jr. *Int. J. Chem. Kinet.* **1981**, *13*, 1133.
(9) Tuazon, E. C.; Atkinson, R.; MacLeod, H.; Biermann, H. W.; Winter, A. M.; Carter, W. P. L.; Pitts, J. N., Jr. *Environ. Sci. Technol.* **1984**, *18*, 981.
(10) Tuazon, E. C.; MacLeod, H.; Atkinson, R.; Carter, W. P. L. *Environ. Sci. Technol.* **1986**, *20*, 383.
(11) Munger, J. W.; Jacob, D. J.; Daube, B. C.; Horowitz, L. W.; Keene, W. C.; Heikes, B. G. *J. Geophys. Res.* **1995**, *100*, 9325.
(12) Lee, Y. N.; Zhou, X.; Hallock, K. *J. Geophys. Res.* **1995**, *100*, 25933.
(13) Raber, W.; Moortgat, G. K. *Progress and Problems in Atmospheric Chemistry*; Barker, J., Ed.; World Scientific: Singapore, 1996; p 318.
(14) Staffelbach, T. A.; Orlando, J. J.; Tyndall, G. S.; Calvert, J. G. *J. Geophys. Res.* **1995**, *100*, 14189.
(15) Tyndall, G. S.; Staffelbach, T. A.; Orlando, J. J.; Calvert, J. G. *Int. J. Chem. Kinet.* **1995**, *27*, 1009.
(16) Plum, C. N.; Sanhueza, E.; Atkinson, R.; Carter, W. P. L.; Pitts, J. N., Jr. *Environ. Sci. Technol.* **1983**, *17*, 479.
(17) Koch, S.; Moortgat, G. K. *J. Phys. Chem. A* **1998**, *102*, 9142.
(18) Meller, R.; Raber, W.; Crowley, J. N.; Jenkin, M. E.; Moortgat, G. K. *J. Photochem. Photobiol., A* **1991**, *62*, 163.
(19) Kyle, E.; Orchard, S. W. *J. Photochem.* **1977**, *7*, 305.
(20) O'Keefe, A.; Deacon, D. A. G. *Rev. Sci. Instrum.* **1988**, *59*, 2544.
(21) O'Keefe, A.; Scherer, J. J.; Cooksy, A. L.; Sheeks, R.; Heath, J.; Saykally, R. J. *Chem. Phys. Lett.* **1990**, *172*, 214.
(22) Zhu, L.; Johnston, G. *J. Phys. Chem.* **1995**, *99*, 15114.
(23) Zhu, L.; Cronin, T.; Narang, A. *J. Phys. Chem. A* **1999**, *103*, 7248.
(24) Cronin, T. J.; Zhu, L. *J. Phys. Chem. A* **1998**, *102*, 10274.
(25) Coveleskie, R. A.; Yardley, J. T. *Chem. Phys.* **1975**, *9*, 277.
(26) Drent, E.; Kommandeur, J. *Chem. Phys. Lett.* **1972**, *14*, 321.
(27) Stoeckel, F.; Schuh, M. D.; Goldstein, N.; Atkinson, G. H. *Chem. Phys.* **1985**, *95*, 135.
(28) Calvert, J. G.; Pitts, J. N., Jr. *Photochemistry*; John Wiley: New York, 1966.
(29) Atkinson, R.; Baulch, D. L.; Cox, R. A.; Hampson, R. F., Jr.; Kerr, J. A.; Troe, J. *J. Phys. Chem. Ref. Data* **1992**, *21*, 1125.
(30) Moortgat, G. K.; Seiler, W.; Warneck, P. *J. Chem. Phys.* **1983**, *78*, 1185.
(31) Cantrell, C. A.; Davidson, J. A.; McDaniel, A. H.; Shetter, R. E.; Calvert, J. G. *J. Phys. Chem.* **1990**, *94*, 3902.
(32) Maric, D.; Burrows, J. P.; Meller, R.; Moortgat, G. K. *J. Photochem. Photobiol. A: Chem.* **1993**, *70*, 205.
(33) Adachi, H.; Basco, N.; James, D. G. L. *Chem. Phys. Lett.* **1978**, *59*, 502.
(34) Parkes, D. A. *Chem. Phys. Lett.* **1981**, *77*, 527.
(35) Demerjian, K. L.; Schere, K. L.; Peterson, J. T. *Adv. Environ. Sci. Technol.* **1980**, *10*, 369.